Decay pathways for protonated and deprotonated Adenine molecules.

L. Giacomozzi,[1] G. D'Angelo,[1,2] S. Diaz-Tendero,[2,3,4] N. de Ruette,[1] M. H. Stockett,[1] M. Alcamí,[2,3,4,5] H. Cederquist,[1] H.T. Schmidt,[1] and H. Zettergren[1]

[1)]*Department of Physics, Stockholm University, Stockholm, SE-106 91, Sweden*[a)]

[2)]*Departamento de Química, Módulo 13, Universidad Autónoma de Madrid, 28049 Madrid, Spain*

[3)]*Condensed Matter Physics Center (IFIMAC), Universidad Autónoma de Madrid, 28049 Madrid, Spain*

[4)]*Institute for Advanced Research in Chemical Sciences (IAdChem), Universidad Autónoma de Madrid, 28049 Madrid, Spain*

[5)]*Instituto Madrileño de Estudios Avanzados en Nanociencia (IMDEA-NANO), 28049 Madrid, Spain*

(Dated: 13 May 2019)

We have measured fragment mass spectra and total destruction cross sections for protonated and deprotonated adenine following collisions with He at center–of– mass energies in the 20-240 eV range. Classical and *ab initio* molecular dynamics simulations are used to provide detailed information on the fragmentation pathways and suggest a range of alternative routes compared to those reported in earlier studies. These new pathways involve, for instance, losses of HNC molecules from protonated adenine and losses of NH_2 or $C_3H_2N_2$ from deprotonated adenine. The present results may be important to advance the understanding of how biomolcules may be formed and processed in various astrophysical environments.

PACS numbers: Valid PACS appear here
Keywords: Suggested keywords

I. INTRODUCTION

It is well-established that energetic particles may cause permanent damage to DNA with severe biological consequences[1,2]. Studies of how DNA–building blocks respond to energetic processing are not only important to advance the understanding of the crucial initial events in radiation damage processes[3–5], but may also shed light on the evolution of biomolecules in extraterrestrial environments[6]. Different possible precursors of nucleobases such as hydrogen cynanide (HCN), pyrimidine ($C_4H_4N_2$), pyridine (C_5H_5N), and imidazole ($C_3H_4N_2$) have been found in dense molecular clouds[6], meteorites[7,8], on surfaces of comets[9,10] and in Titan's atmosphere[6,11]. However, the detection of nucleobases still remains elusive. Adenine ($C_5H_5N_5$) is the most stable nucleobase[12], which makes it the most likely candidate to survive in such environments[6]. It may be viewed as five fused HCN units or as pyrimidine ($C_4H_4N_2$) fused to an imidazole ring ($C_3H_4N_2$), see Fig. 1. Related bottom–up formation processes have been suggested as possible pathways in the interstellar medium (ISM) or during the early stages of Earth's evolution[6,13–15]. However, several studies have shown that adenine formation through HCN pentamerization[13,14] involves large reaction barriers, and requires photoactivation[14], ammonia or water catalysis[13] to occur. Possible adenine precursors could instead be C_3NH and $HNCNH/H_2NCN$, as a recent theoretical study suggests[15].

Collision Induced Dissociation (CID) experiments in combination with theoretical calculations have been suggested as a tool to study the molecular formation process in reverse[6] and may thus provide information on for instance biomolecular precursors. Previous CID studies have shown that positively charged adenine molecules (protonated and radical cations) predominantly decay by sequential losses of HCN[16–19]. Other important fragmentation channels include the loss of ammonia (NH_3)[16–19] and NCHNH/HNCNH[16,18,20]. Similarly, fragmentation of deprotonated adenine mainly proceed through losses of HCN and NCHNH/HNCNH[6,20]. These studies unambiguously show that adenine is a source of HCN and a rich variety of small (nitrogen containing) hydrocarbons when energetically processed. However, the actual destruction pathways leading to specific molecular structures have not yet been fully unraveled.

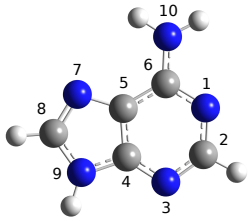

FIG. 1. The most stable Adenine structure[6], where the nitrogens are shown in blue, the carbons in grey and the hydrogens in white.

In this paper, we provide new detailed information on the fragmentation dynamics of protonated and deprotonated adenine through CID experiments, molecular structure calculations, as well as classical and *ab initio* molecular dynamics simulations. Here, the nucleobases collide with He at center–of–mass energies in the 20–240 eV range. This corresponds to typical conditions in supernova shock-waves[21]

[a)]Electronic mail: linda.giacomozzi@fysik.su.se

where complex molecules such as Polycyclic Aromatic Hydrocarbons (PAHs) are processed by energetic ions/atoms. In Sec. II we present the experimental techniques used to record fragmentation mass spectra and the total absolute fragmentation cross sections in such collisions. The computational tools are introduced in Sec. III. We use classical molecular dynamics simulations to determine the energy deposited in the collisions, *ab initio* molecular dynamics simulations to follow the decay pathways, and molecular structure calculations to explore the potential energy surfaces for specific fragmentation pathways. In Sec. IV we compare measured and simulated mass spectra for both protonated and deprotonated adenine, and discuss the mechanisms leading to the most prominent decay pathways according to our ab–initio molecular dynamics simulations. These include, to our knowledge, a range of new pathways of potential importance for the life-cycle of adenine and other complex molecular systems in *e.g.* astrophysical environments.

II. EXPERIMENTAL TECHNIQUES

The experiments were carried out using the accelerator mass spectrometer located in the Electrospray Ion Source Laboratory (EIS-LAB)[22] at the DESIREE infrastructure[23,24], Stockholm University. In fig. 2 we show a schematic of the setup. A complete description of the apparatus can be found elsewhere[22].

Adenine was purchased from Sigma-Aldrich and dissolved in a solution specific to the charge state of interest. In the case of protonated Adenine, the sample was dissolved in a solvent of Methanol : Water : Acetic Acid (47.5% : 47.5% : 5% by volume), while for the deprotonated Adenine, the solvent was Methanol : Acetonitrile (20% : 80% in volume) and a small amount of Ammonium Hydroxide. These solutions were used to produce the corresponding gas phase molecular ions with the aid of an ElectroSpray Ionization (ESI) source coupled to a heated capillary (see Fig. 2). The formed bare ions passed through a radio-frequency ion funnel, an octupole trap, an octupole guide and a quadrupole mass filter for mass–to–charge selection. Once the desired ions were selected, they were accelerated to a kinetic energy in the 0.7-8.4 keV range and steered through a 40 mm long gas cell, where the ions collided with He gas at center–of–mass energies, E_{CM}, of 20-240 eV. The charged fragments formed in the collisions were guided by a set of lenses and analyzed by means of an electrostatic energy analyzer. The kinetic energy-to-charge spectrum was recorded by registering the position of each ion hit on a position sensitive micro-channel plate detector as a function of the analyzer voltage. Assuming the fragments have approximately the same velocity as the parent ions before the collision, this spectrum is readily converted to a mass-to-charge spectrum. The destruction cross section was measured by monitoring the intensity of the primary beam as a function of the pressure in the gas cell, which was measured by means of a capacitance manometer[22].

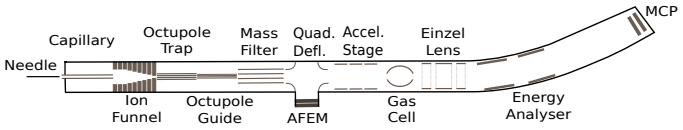

FIG. 2. Schematic of the experimental apparatus used for Collision Induced Dissociation (CID) experiments[22] (not to scale).

III. COMPUTATIONAL DETAILS

We performed classical molecular dynamics (MD) simulations of collisions between neutral He and an isolated adenine molecule to determine the amount of energy deposited in the collisions and to investigate the importance of prompt atom knockout processes[25]. These simulations were carried out using the LAMMPS packages[26], following the approach successfully used for collisions involving PAHs[27–29], fullerenes[30,31], and their clusters[25,32,33]. The interactions between the incoming He projectile and each atom of the target adenine molecule were described using the ZBL (Ziegler-Biersack-Littmark) potential, while the reactive Tersoff potential was used to model the target intramolecular bonds. In the simulations, the He atom is given a randomly selected initial trajectory towards a randomly oriented adenine molecule. The collision dynamics is followed for 10 ps and repeated 10000 times for a given collision energy. We determine the energy deposited in the collision from the kinetic energy loss of the He-projectile. Furthermore, we calculate the cross sections for heavy atom (carbon or nitrogen) knockouts in Rutherford-like scattering processes by analysing the fragments formed in the collisions[27]. This has been shown to be an important non-statistical fragmentation pathway for stable and large molecular systems such as PAHs[27–29], clusters[25,32,33] and porphyrins[34] in the velocity range considered here. The present model has been shown to overestimate the threshold energy for prompt atom knockout in collisions with helium[35]. To compensate for this, the model destruction cross sections are multiplied by a factor 4/3 as established from previous studies of PAHs[35].

We carried out *ab initio* molecular dynamics (AIMD) simulations to model statistical fragmentation processes following redistribution of the excitation energy across all vibrational degrees of freedom of the molecule in its electronic ground state. Here, we used the Atom-centered Density Matrix Propagation method (ADMP)[36–38], employing the B3LYP functional together with the 6-31++G(d,p) basis set. In these simulations, we used a time step $\Delta t = 0.5$ fs, a fictitious mass of $\mu = 0.1$ amu to minimize the loss of adiabaticity[39], a maximum simulation time of 4.0 ps and values of internal vibrational energy in the 10-30 eV range. The simulations were performed up to full convergence of the electronic structure at each time step to preserve the adiabaticity of the system (Born-Oppenheimer approximation). Statistics were carried out over the computed trajectories, where the kinetic energy was randomly distributed over the nuclear degrees of freedom.

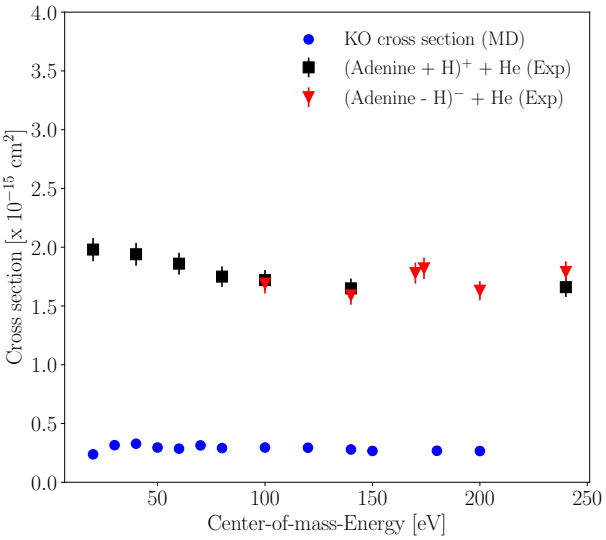

FIG. 3. Absolute total fragmentation cross sections for protonated adenine (black squares), deprotonated adenine (red triangles) as a function of the center–of–mass collision energy. The corresponding heavy atom knockout (KO) cross section from classical molecular dynamics simulations (blue dots) is reported.

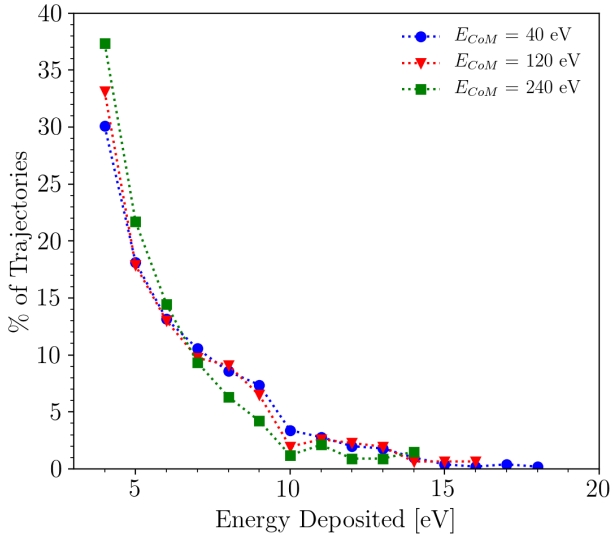

FIG. 4. Energy transfer distributions from classical molecular dynamics simulations of adenine colliding with He at 40 eV (blue dots), 120 eV (red triangles) and 240 eV(green squares) in the center–of–mass frame. Prompt atom knockout processes are excluded.

Finally, DFT molecular structure optimizations, transition state (TS) searches and intrinsic reaction coordinate (IRC) calculations were performed at the B3LYP/6-311++G(d,p) level of theory to further explore parts of the potential energy surfaces (PES) for a few important fragmentation pathways observed in the *ab initio* MD simulations. The molecular structure calculations and the *ab initio* MD calculations were performed using the Gaussian 09 program[40]. The combination of *ab initio* molecular dynamics simulations with further exploration of the potential energy surface has been shown to be a very efficient computational strategy to provide theoretical insight into the fragmentation of charged and excited biomolecules induced by collisions with ions[41–44].

IV. RESULTS AND DISCUSSIONS

A. Destruction cross sections and energy transfer distribution

In fig. 3, we show the measured destruction cross sections for protonated adenine (black squares) and deprotonated adenine (red triangles) as functions of the center–of–mass collision energies in the 20 to 240 eV range. The experimental cross sections are around 1.8 $\times 10^{-15}$ cm^{-2} independent of the collision energy and the charge of the projectile within the present parameter ranges. This suggests that the overall stability is similar for deprotonated and protonated adenine molecules.

Previous studies[27,34,45] have shown that single or multiple atoms may be knocked out in atom-molecule collisions. The interplay between such prompt non-statistical fragmentation processes and statistical relaxation processes depends sensitively on the collision velocity, the atomic projectile mass and the stability of the target molecule. At center–of–mass collision energies of a few tens of eV, atom knockout may become the dominant decay pathway for large molecules, as demonstrated for PAHs[27,46]. In the present case, the heavy atom knockout cross section is about 15% of the total fragmentation cross section according to our molecular dynamic simulations (blue dots in Fig. 3). This suggests that statistical fragmentation is the dominant decay pathway for adenine in the present energy range. In such cases, the molecule is left intact on the short (ps) MD-simulation timescales but sufficient amount of energy has been deposited in the collision for fragmentation to occur on experimental (μs) timescales.

From the classical molecular dynamics simulations we extract the energy deposited for those collisions leaving intact molecules on the ps simulation timescales and may lead to statistical fragmentation on longer (experimental) timescales. These are shown in Fig. 4 for center–of–mass collision energies of 40 eV (blue dots), 120 eV (red triangles) and 240 eV (green squares). The energy distributions are similar in all three cases and extend up to about 18 eV, *i.e.* well above the dissociation energies (about 5 eV) for protonated[47] and deprotonated adenine[6]. This is consistent with the observed nearly constant total fragmentation cross sections as shown in Fig. 3.

B. Decay pathways for Protonated Adenine

We observe rich fragmentation mass spectra when protonated adenine collides with He in the present collision energy range. This is illustrated in the upper panel of Fig. 5 for which the center–of–mass collision energy is 240 eV. We observe the same peaks but with different intensity ratios compared to those reported earlier for collisions with neutral gases at low collision energies (below 5 eV in the center–of–mass frame)[16,18–20] as well as at higher collision energies (around 1 keV in the center–of–mass frame)[48]. Furthermore, we observe peaks that to our knowledge have not been reported in the literature, which will be discussed in more detail below.

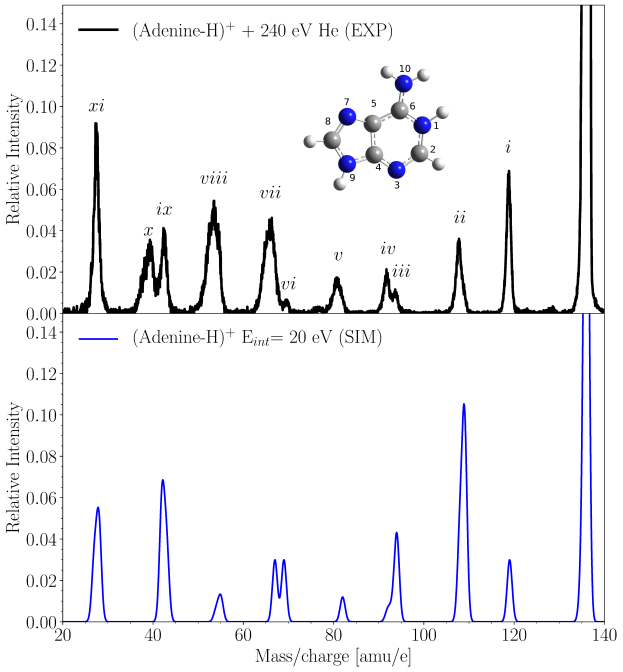

FIG. 5. Top panel: Experimental mass spectrum for protonated Adenine colliding with He at 240 eV in the center–of–mass frame. Bottom panel: Fragmentation mass spectrum for protonated adenine from *ab initio* molecular dynamic simulations. The internal energy (E_{int}) was set to 20 eV (bottom panel). The peaks in the simulated spectrum have been convoluted with a gaussian function to reproduce the widths of the experimental peaks.

The lower panel of Fig. 5 shows the results from the *ab initio* MD simulations when 20 eV energy is deposited into the protonated adenine molecule. This is somewhat higher than the typical energy deposited in the collisions according to our classical MD simulations (see Fig. 4), but is needed to induce fragmentation on the simulation timescale. As a consequence

Peak	Charged fragment	Mass [amu]	Neutral fragments	Ref
i	$C_5H_3N_4^+$	119	NH_3	16,18–20,48
ii	$C_4H_5N_4^+$	109	HCN	16,18–20,48
ii	$C_4H_4N_4^+$	108	HCNH H + HCN	48
iii	$C_4H_4N_3^+$	94	HNCNH	16,18,20
iv	$C_4H_2N_3^+$	92	CH_4N_2	16,19,20
v	$C_3H_4N_3^+$	82	HCN + HNC 2HCN	16,18–20,48
vi	$C_2H_3N_3^+$	69	$C_3H_3N_2$	
vii	$C_3H_3N_2^+$	67	HCN + HNCNH NH_3 + C_2N_2	16,18,19,48 16,18
viii	$C_2H_3N_2^+$	55	2HCN + HNC 3HCN	16,18–20,48
viii	$C_3H_4N_3^+$	54	2HCN + HCNH	
ix	$CH_3N_2^+$	43	$H_2C_3N_2$ + HCN $C_4H_3N_3$	48
ix	$CH_2N_2^+$	42	$C_3H_3N_2$ + HCN	
x	$C_2H_2N^+$	40 (*)	HNCNH + 2HCN NH_3 + C_2N_2 + HCN	16,18 16
xi	$HCNH^+$	28	HNCNH + $C_3H_2N_2$ 4HCN	16,18,20,48
xi	HCN^+	27	HNC + HNCNH + $C_2H_2N_2$	

TABLE I. Assignment of experimental peaks in the mass spectrum for protonated adenine shown in the upper panel of Fig. 5 with the aid of the results from the present *ab initio* molecular dynamics simulations and results reported in the literature. The peak labeled (*) is observed in the experiments, but not in the *ab initio* molecular dynamics simulations.

of the different timescales probed in the experiments and in the simulations, it is not possible to compare the fragment peak intensity distribution (*i.e.* branching ratios). However, as all fragmentation peaks observed in the simulated spectrum are also seen in the experiment, we assign the decay pathways responsible for the different peaks in the measured mass spectrum (upper panel of Fig 5) to those that appear in the simulations.

In Table I, we list the experimental peaks labelled by the letters as shown in Fig 5 together with the corresponding fragmentation channels observed in the *ab initio* MD simulations. In Fig. 6 we show snapshots from a selection of six of these different pathways. We attribute the peak labelled by *i* in the experimental mass spectrum to the loss of NH_3 (see Fig. 5). Our *ab initio* MD-simulations (see pathway *i* in Fig. 6) agree with previous studies[16,18–20,48] and show that this fragmentation pathway involves hydrogen migration from N1 to N10 (see the inset in Fig. 5). The energy required for this channel is 3.93 eV according to our molecular structure calculations (see the Supplementary Information), which is significantly lower compared to NH_2-loss (5.23 eV) through direct cleavage of the C6-N10 bond. This explains why NH_2-loss is not an important decay pathway for protonated adenine.

The *ab initio* MD simulations suggest that HCN-loss (pathway *ii*) may be initiated by opening of the six-membered ring between N1 and C2, followed by cleavage of the N3-C4 bond

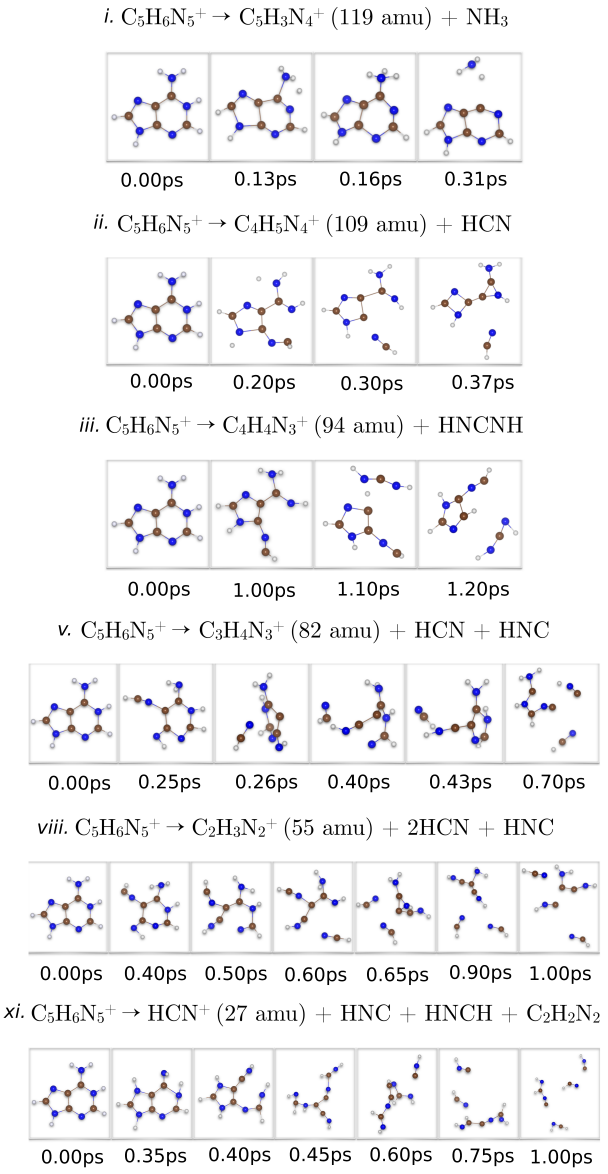

FIG. 6. Snapshots from *ab initio* molecular dynamics simulations for a selection of fragmentation pathways for protonated Adenine. The pathways are labelled by the nubers corresponding to the different peaks they contribute to in the mass spectrum (see Fig. 5).

(see Fig. 6). This pathway is different compared to those suggested by Nelson *et al.*[16], where HCN-loss involves either a H migration that initiates the ring opening or a direct cleavage of the N1-C6 bond. We find that the first step towards HNCNH-loss (pathway *iii*) is the same as for HCN-loss (see Fig. 6), which in this case is followed by cleavage of the N1-C6 bond. This is in agreement with the results from isotope labelling studies[16,20].

The fragment peak at 82 amu ($C_3H_4N_3^+$) has in earlier studies been assigned to sequential loss of two HCN fragments[16,18–20,48]. Our calculations suggest an alternative pathway corresponding to the loss of one HCN and one HNC molecule, as shown in Fig. 6 (pathway *v*). Similarly, the peak at 55 amu (pathway *viii*), may be due to the loss of two HCN and one HNC molecules rather than losses of three HCN molecules as reported earlier[16,18–20,48]. The detection of the fragment peak at 27 amu (HCN^+) has been previously identified to stem from the loss of four HCN molecules[16,18–20,48]. However, our *ab initio* MD simulations suggest that this fragment stems from the loss of HNC, HNCH and $C_2H_2N_2$ (pathway *xi* in Fig.6).

In the experiment, we observe fragments with a mass–to–charge ratio of 40 amu (see Fig. 5, top panel) that are not seen in the simulated mass spectrum. Previous studies[16,48] have considered this fragment as resulting from the loss of HCN from the fragment at 67 amu. Such secondary fragmentation processes are likely to occur on longer timescales than those probed in our simulations.

C. Decay pathways for Deprotonated Adenine

In the top panel of Fig. 7, we show the mass spectrum of negative fragments following collisions between deprotonated adenine and He at 240 eV collision energy in the center–of–mass frame. The spectrum was recorded with the same experimental conditions regarding the ion beam intensity, target gas pressure and measurement time, as in the case of protonated adenine (Fig. 5). However, the anionic fragment yield is much lower, even though the total destruction cross sections are similar for protonated and deprotonated adenine (see Fig. 3). This suggests that electron loss is likely to occur in the deprotonated case, such that only a small fraction of the charged fragments survive.

Our simulated mass spectrum for internally heated (E_{int}=15 eV) deprotonated adenine is shown in the lower panel of Fig. 7. As in the protonated case, the same peaks appear in the simulated mass spectrum as in the experimental one. Again the branching ratios are different, which we attribute to the different experimental and simulation timescales. In Table II, we show the fragmentation pathways from the simulations corresponding to the different peaks in the measured mass spectrum (upper panel of Fig. 7) and the pathways reported from low energy collisions (around 3 eV) with helium[6] and for 5 to 25 eV collisions with argon[20]. Cole *et al.*[6] showed that deprotonated adenine predominately decays by loosing HCN (pathway *ii*) or HNCNH (pathway *iii*). A strong peak at 26 amu was observed by Kamel *et al.* when deprotonated molecule was generated from the dissociation of vidarabine ($C_{10}H_{13}N_5O_4$)[20]. Interestingly, we observe a peak at 118 amu (pathway *i*) which is not seen in these earlier measurements[6,20]. We attribute this peak to NH_2-loss as the activation energy for this channel (4.11 eV) is significantly lower compared to NH_3-loss (4.75 eV) according to our molecular stucture calculations (see the Supplementary Information). Our *ab initio* MD simulations support this scenario, as can be seen in the snapshots for pathway *i* shown in Fig. 8. In the same figure, we show snapshots for several other observed fragmentation pathways. These show that HCN-loss may be initiated by opening of the five-membered ring rather than through opening of the six-membered ring[6] (pathway *ii*). This

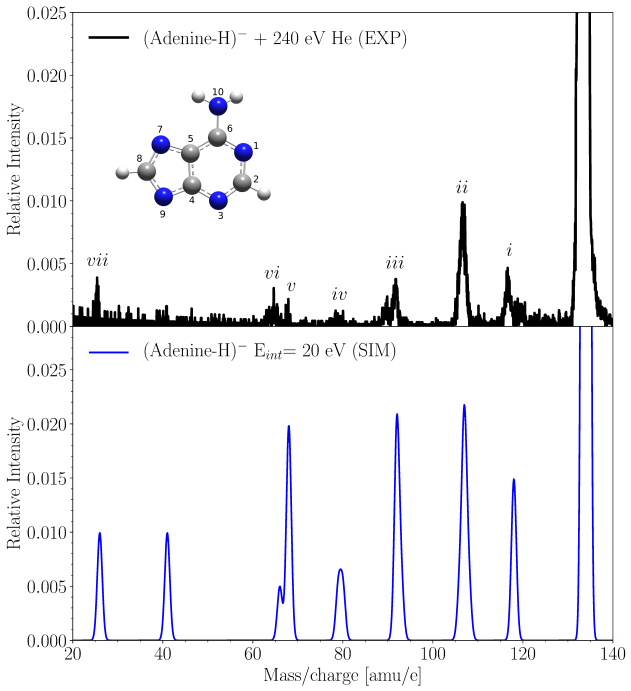

FIG. 7. Top panel: Experimental mass spectrum of deprotonated Adenine in collision with He at 240 eV in the center–of–mass energy. Bottom panel: Fragmentation mass spectrum of deprotonated adenine from *ab inito* molecular dynamic simulations. The internal energy (E_{int}) was set to 15 eV. The peaks in the simulated mass spectrum have been convoluted with a gaussian function to reproduce the widths of the experimental peaks.

Peak	Charged fragment	Mass [amu]	Neutral fragments	Ref
i	$C_5H_2N_4^-$	118	NH_2	
ii	$C_4H_4N_4^-$	108	CN	
ii	$C_4H_3N_4^-$	107	HCN	6,20
ii	$C_4H_2N_4^-$	106	HCNH	
iii	$C_4H_3N_3^-$	93	HNCN	
iii	$C_4H_2N_3^-$	92	HNCNH	6,20
iv	$C_3N_3^-$	80	2HCN	
iv	$C_3HN_3^-$	79	HCN + H_2CN	
v	$C_2H_2N_3^-$	68	$C_3H_2N_2$	
vi	$C_3H_2N_2^-$	66	HCN +CHN_2	
vii	CN^-	26	HNC + $C_3H_3N_3$	20

TABLE II. Assignments of experimental peaks in the mass spectrum of deprotonated adenine shown in the upper panel of Fig. 7 with the aid of the results from *ab initio* molecular dynamics simulations and results reported in the literature.

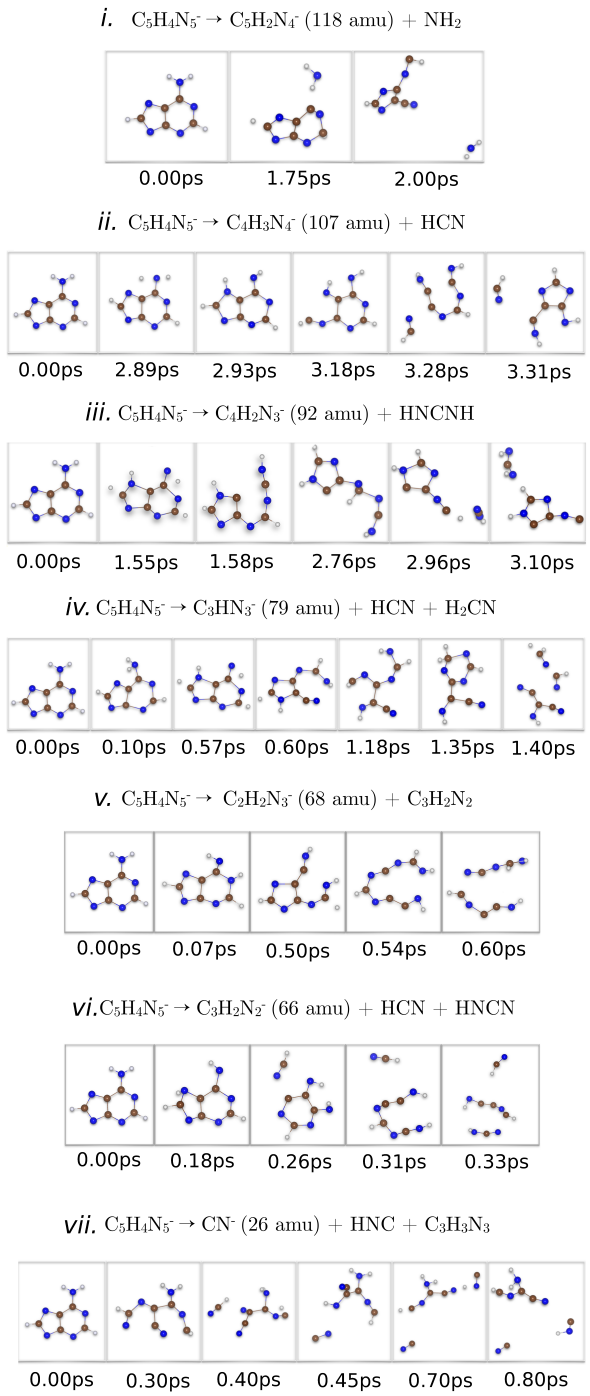

FIG. 8. Snapshots from *ab initio* molecular dynamics simulations for a selection of fragmentation pathways of deprotonated Adenine. The pathways are labelled by the numbers corresponding to the different peaks they contribute to Fig. 7.

latter fragmentation pathway has been proposed as a plausible reverse route to the formation of adenine[13,14], and thus, our results suggest a possible alternative formation pathway.

The *ab initio* MD simulations suggest that the fragments having masses 79, 68 and 66 amu (pathways *iv*-*vi*) are initiated by hydrogen migration from N10 to other atoms in the depro-

tonated adenine molecule (see Fig. 8). The former is attributed to $C_3HN_3^-$ for which the two hydrogens on N10 have migrated to N1 and C6, followed by the opening of both rings and losses of HCN and H_2CN. The peak at 68 amu ($C_2H_2N_3^-$) is due to one hydrogen migrating from N10 to N1, which induces the 6-membered ring to open and the molecule to loose C_3H_2N. The peak at 66 amu ($C_3H_2N_2^-$) is formed through hydrogen migration to N7 causing the loss of HCN from the five-membered ring and loss of CHN_2 from the 6-membered ring. The latter two fragmentation processes are similar to those observed for protonated adenine yielding the peaks at 69 amu ($C_2H_3N_3^+$) and 67 amu ($C_3H_3N_2^+$), respectively (see Fig. 5). Finally, our *ab initio* MD simulations suggest that CN^- (26 amu), HNC and $C_3H_3N_3$ are formed due to direct cleavages of the N3-C2 and C4-N9 bonds (pathway *vii* in Fig. 8).

V. SUMMARY AND CONCLUSIONS

In the present work we have studied the fragmentation of protonated and deprotonated adenine following collisions with He in the 20-240 eV center–of–mass energy range. We find that the destruction cross section is constant and independent of the charge carrier in this energy window. This is due to their similar binding energies and small differences in energy deposition above the threshold energy required to induce statistical fragmentation processes. Our classical molecular dynamics simulations show that prompt atom knockout is responsible for minor fractions (up to 15 %) of the total destruction cross sections, and that the fragmentation mass spectra are thus predominantly due to statistical fragmentation processes.

Ab initio molecular dynamics simulations were used to model such processes and we found that all peaks in the simulated mass spectra appear in the corresponding experimental ones. The simulations provide detailed information on the fragmentation mechanisms and were used to identify both the charged and neutral final products. These show that the fragmentation of protonated and deprotonated adenine may follow alternative pathways than those previously reported and discussed as possible routes to the formation and destruction of nucleobases in space[6,13–16,18–20,48]. For instance, fragmentation of protonated adenine may involve the loss of both HNC and HCN rather than multiple HCN-loss[16,18–20,48]. For deprotonated adenine, we report fragmentation pathways which, to our knowledge, have not been discussed before in the literature[6,20], *e.g.* loss of NH_2, $C_3H_2N_2$ or the formation of CN^-. The present combined experimental and computational approach may be used as a tool to reveal the decay pathways and possible precursors for other (bio)molecular systems, and to gauge their significance in various environments including astrophysical ones.

ACKNOWLEDGMENTS

This work was supported by the Swedish Research Council (Constant Nos 2017-00621, 2015-04990, 2016-04181, 2018-04092). Furthermore, we acknowledge the European Joint on Theoretical Chemistry and Computational Modelling (INTEJD-TCCM). We acknowledge the generous allocation of computer time at the Centro de Computacion Cientifica at the Universidad Autonoma de Madrid (CCC-UAM). This work was partially supported by the project CTQ2016-76061-P of the Spanish Ministerio de Economia y Competitividad (MINECO).

[1] K. K. Khanna and S. P. Jackson, Nature Genetics **27**, 247 (2001).
[2] M. A. Huels *et al.*, Journal of the American Chemical Society **125**, 4467 (2003).
[3] B. Boudaïffa *et al.*, Science **287**, 1658 (2000).
[4] X. Pan *et al.*, Phys. Rev. Lett. **90**, 208102 (2003).
[5] F. Martin *et al.*, Phys. Rev. Lett. **93**, 208 (2004).
[6] C. A. Cole *et al.*, The Journal of Physical Chemistry A **119**, 334 (2015).
[7] Z. Martins *et al.*, Earth and Planetary Science Letters **270**, 130 (2008).
[8] M. P. Callahan *et al.*, Proceedings of the National Academy of Sciences **108**, 13995 (2011).
[9] J. Kissel and F. R. Krueger, Nature **326**, 755.
[10] S. Chakraborty *et al.*, International Journal of Quantum Chemistry **118**, e25459 (2017).
[11] S. Pilling *et al.*, The Journal of Physical Chemistry A **113**, 11161 (2009).
[12] B. Pullman and A. Pullman, Nature **198**, 1225 (1962).
[13] D. Roy, K. Najafian, and P. von Rague Schleyer, Proceedings of the National Academy of Sciences **104**, 17272 (2007).
[14] R. Glaser *et al.*, Astrobiology **7**, 455 (2007).
[15] K. M. Merz Jr., E. C. Aguiar, and J. B. P. da Silva, The Journal of Physical Chemistry A **118**, 3637 (2014).
[16] C. C. Nelson and J. A. McCloskey, Journal of the American Chemical Society **114**, 3661 (1992).
[17] S. Sethi *et al.*, Journal of the American Chemical Society **104**, 3349 (1982).
[18] M. Qian *et al.*, Journal of the American Society for Mass Spectrometry **18**, 2040 (2007).
[19] A. J. Alexander *et al.*, Analytical Chemistry **59**, 2484 (1987).
[20] A. M. Kamel and B. Munson, European Journal of Mass Spectrometry **10**, 239 (2004).
[21] E. R. Micelotta, A. P. Jones, and A. G. G. M. Tielens, Astronomy and Astrophysics **510**, A36 (2010).
[22] N. de Ruette *et al.*, Review of Scientific Instruments **89**, 075102 (2018).
[23] H. T. Schmidt *et al.*, Review of Scientific Instruments **84**, 055115 (2013).
[24] R. D. Thomas *et al.*, Review of Scientific Instruments **82**, 065112 (2011).
[25] R. Delaunay *et al.*, The Journal of Physical Chemistry Letters **6**, 1536 (2015).
[26] S. Plimpton, Journal of Computational Physics **117**, 1 (1995).
[27] M. H. Stockett *et al.*, Physical Review A **89**, 032701 (2014).
[28] M. H. Stockett *et al.*, J. Phys. Chem. Lett. **6**, 4504 (2015).
[29] M. Gatchell *et al.*, Physical Review A **92**, 050702 (2015).
[30] H. Zettergren *et al.*, Phys. Rev. Lett. **110**, 185501 (2013).
[31] Y. Wang *et al.*, Phys. Rev. A **89**, 062708 (2014).
[32] M. Gatchell *et al.*, Phys. Chem. Chem. Phys. **19**, 19665 (2017).
[33] R. Delaunay *et al.*, The Journal of Physical Chemistry Letters **6**, 1536 (2015).
[34] L. Giacomozzi *et al.*, Phys. Chem. Chem. Phys. **19**, 19750 (2017).
[35] M. H. Stockett *et al.*, Phys. Chem. Chem. Phys. **16**, 21980 (2014).
[36] H. B. Schlegel *et al.*, The Journal of Chemical Physics **114**, 9758 (2001).
[37] S. S. Iyengar *et al.*, The Journal of Chemical Physics **115**, 10291 (2001).
[38] H. B. Schlegel *et al.*, The Journal of Chemical Physics **117**, 8694 (2002).
[39] S. S. Iyengar, H. B. Schlegel, J. M. Millam, G. A. Voth, G. E. Scuseria, and M. J. Frisch, The Journal of Chemical Physics **115**, 10291 (2001).
[40] M. J. Frisch *et al.*, "Gaussian 09 revision e.01," Gaussian Inc. Wallingford CT 2009.
[41] S. Maclot, D. G. Piekarski, A. Domaracka, A. Méry, V. Vizcaino, L. Adoui, F. Martín, M. Alcamí, B. A. Huber, P. Rousseau, and S. Díaz-Tendero, J. Phys. Chem. Lett. **4**, 3903 (2013).
[42] S. Maclot, R. Delaunay, D. G. Piekarski, A. Domaracka, B. A. Huber, L. Adoui, F. Martín, M. Alcamí, L. Avaldi, P. Bolognesi, S. Díaz-Tendero, and P. Rousseau, Phys. Rev. Lett. **117**, 073201 (2016).
[43] D. G. Piekarski, R. Delaunay, S. Maclot, L. Adoui, F. Martín, M. Alcamí,

B. A. Huber, P. Rousseau, A. Domaracka, and S. Díaz-Tendero, Physical Chemistry Chemical Physics **17**, 16767 (2015).
[44]D. G. Piekarski, R. Delaunay, A. Mika, S. Maclot, L. Adoui, F. Martín, M. Alcamí, B. A. Huber, P. Rousseau, S. Díaz-Tendero, and A. Domaracka, Physical Chemistry Chemical Physics **19**, 19609 (2017).
[45]M. Gatchell and H. Zettergren, Journal of Physics B: Atomic, Molecular and Optical Physics **49**, 162001 (2016).
[46]T. Chen *et al.*, The journal of Chemical Physics **140**, 224306 (2014).
[47]F. Turecček and X. Chen, Journal of the American Society for Mass Spectrometry **16**, 1713 (2005).
[48]X. Chen *et al.*, The Journal of Physical Chemistry A **108**, 9283 (2004).
[49]S. Thomas *et al.*, ChemPhysChem **7**, 2339 (2006).
[50]J. de Vries *et al.*, Phys. Rev. Lett. **91**, 053401 (2003).
[51]J.-C. Poully *et al.*, Phys. Chem. Chem. Phys. **17**, 7172 (2015).
[52]S. Pilling *et al.*, Proceedings of the International Astronomical Union **4**, 371–376 (2008).
[53]Y.-J. Kuan *et al.*, Monthly Notices of the Royal Astronomical Society **345**, 650 (2003).
[54]H.-W. Jochims *et al.*, Chemical Physics **314**, 263 (2005).
[55]J. M. Rice and G. O. Dudek, Journal of the American Chemical Society **89**, 2719 (1967).
[56]B. F. Minaev *et al.*, The Journal of chemical physics **140**, 175101 (2014).
[57]J. Tabet *et al.*, International Journal of Mass Spectrometry **292**, 53 (2010).
[58]L. Sadr-Arani *et al.*, Physical Chemistry Chemical Physics **17**, 11813 (2015).
[59]J. Tersoff, Phys. Rev. B **37**, 6991 (1988).
[60]J. F. Ziegler and J. P. Biersack, "The stopping and range of ions in matter," in *Treatise on Heavy-Ion Science: Volume 6: Astrophysics, Chemistry, and Condensed Matter*, edited by D. A. Bromley (Springer US, Boston, MA, 1985) pp. 93–129.
[61]A. D. Becke, The Journal of Chemical Physics **98**, 1372 (1993).
[62]C. Lee, W. Yang, and R. G. Parr, Phys. Rev. B **37**, 785 (1988).
[63]D. Marx and J. Hutter, *Ab Initio Molecular Dynamics: Basic Theory and Advanced Methods* (Cambridge University Press, 2009).
[64]D. Huber *et al.*, The Journal of chemical physics **125**, 084304 (2006).